Prediction of Mine Face Ventilation using Computational Fluid Dynamics

University of Kentucky

October 6, 2003

Introduction

The objective of this document is to update NIOSH on the progress that has been made in the past year with respect to CFD predictions of mine face ventilation cases using commercial software. Several studies will be presented including a comparison of Fluent with CFX for all four scenarios discussed in the previous years report, modeling of a cylindrical scrubber within the mine and simulations of a the flow around a continuous miner, with scrubbers on-board, at the cutting face.

Comparing Fluent to CFX

A comparison of Fluent and CFX was performed by simulating the four scenarios presented in last years report. To eliminate variation in grid generation and refinement an external software, GridPro, was utilized to generate all the grids in this study. GridPro is an automatic grid generator which yields a structured grid that can be imported directly into both of the solvers mentioned above. Three grids for each scenario (coarse, moderate, fine) were computed using both Fluent and CFX in an effort to find a grid-independent solution. The results of said solutions are presented in this section.

Baseline PIV Results

Dr's. Andrzej M. Wala and Jamey D. Jacob of the departments of Mining and Mechanical Engineering, respectively, performed the PIV experiments of each scenario using a 1:15 scale model of a mine face. The results of these experiments, figures 1 through 4, will be used as the baseline for our simulations. In three of the four cases, an onset separation can be seen where flow reverses before reaching the face. This separation is driven by an adverse pressure gradient which builds up as the width of the mine decreases. The κ-ω SST (Shear Stress Transport) turbulence model is was selected for its ability to accurately predict separation due to adverse pressure gradients.

Figure 1: Velocity vectors and contours from PIV experiments for 30 Foot Box Cut

Figure 2: Velocity vectors and contours from PIV experiments for 30 Foot Slab Cut

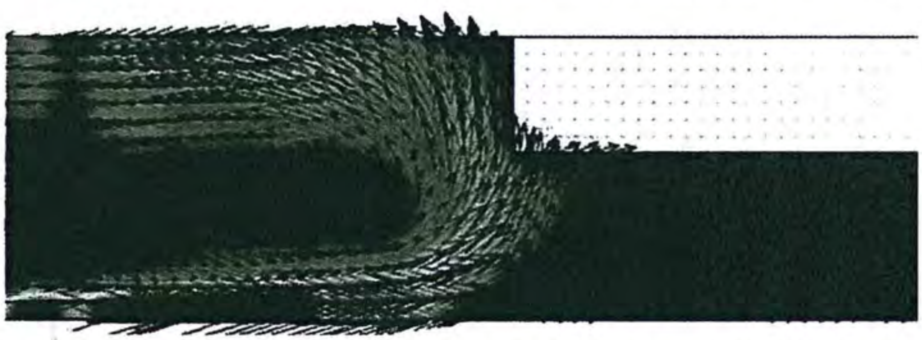

Figure 3: Velocity vectors and contours from PIV experiments for 60 Foot Box Cut

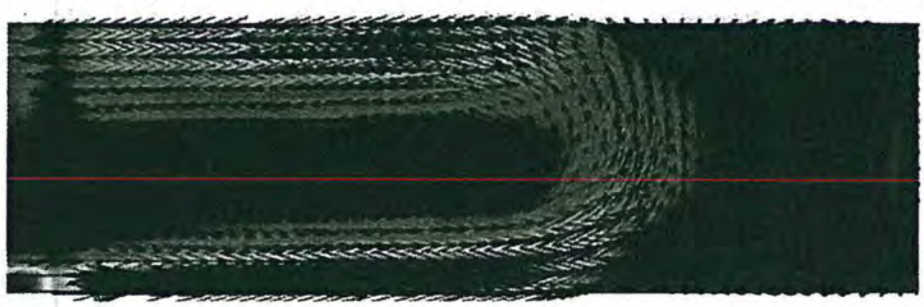

Figure 4: Velocity vectors and contours from PIV experiments for 60 Foot Slab Cut

CFD Results

30 Foot Box Cut

In the scenario for the 30 foot box cut an onset separation develops only a few feet downstream from the end of the curtain at the beginning of the slab. This flow separation produces a low velocity recirculation of air deep into the mine. In an actual mine, this flow pattern could allow dangerous levels of methane gas to build near the cutting face. Although the introduction of methane gas to the flow is not being simulated here, a correlation between flow patterns containing air only and air with methane is assumed. Figures 5, 6 and 7 illustrate the results yielded by Fluent and CFX for the three grid densities (coarse, moderate and fine). Comparing these results to the baseline results, figure 1, one can see that Fluent predicts the desired characteristics independent of grid density. Although, the moderate and fine grid results for CFX correctly predict the separation point, the coarse grid solution did not. Thus, some confidence in the CFX solutions is lost. However, since the finer grids yield a proper solution, one could make the argument that this is the grid-independent solution for CFX.

30 Foot Slab Cut

In the 30 foot slab cut scenario no onset separation occurs as that flow carries entirely to the face before redirecting. Simulating this scenario tests the codes ability to decipher a difference between flows with and without separation. Although it is known that predicting a flow field without separation is much easier, the code must be able to predict the flow field with the same method used for the flow fields with separation. This is especially important since the CFD tools in question may be used to develop and optimize mining techniques and setups. Comparing the solutions in figures 8, 9 and 10 to the PIV result illustrated in figure 2 similar flow patterns are found. Noticing that for all three grid levels the flow carries to the mine face before turning, one can confirm that both codes predict an accurate grid-independent solution.

60 Foot Box Cut

In the 60 foot box cut scenario onset separation occurs at the beginning of the slab as shown in figure 3. As in the 30 foot box cut, this separation generates a low velocity recirculation of air deep into the mine. If this flow field were generated during normal operation of a real mine, dangerous levels of methane could collect near the cutting face. In figures 11, 12 and 13, it is shown that both codes predict the separation in the proper location for the coarse, moderate and fine grid cases. Therefore, one can claim that the grid-independent solution generated by both codes is accurate for this scenario.

60 Foot Slab Cut

The 60 foot slab cut scenario occurs when the mine is cut to full width, 20 feet, and 60 feet deep. One may expect the flow field to resemble that of the 30 foot slab cut since such a resemblance was seen for the two box cut cases. However, an interesting result is found for the scenario in question when one views the PIV result illustrated in figure 4. A late separation of the flow occurs in the mine roughly 20 feet shy of the cutting face. As seen in figures 14, 15 and 16, both codes had difficulty predicting this flow field. Due to the highly unstable nature of the flow, an accurate steady-state simulation of flow structure was not feasible. The codes' inability to generate a converged solution yielded variation in the results. Although less variation was seen in Fluent's prediction of the flow structure, neither code was able to produce converged, accurate solutions for this scenario. One suggestion may be to approach the problem from a transient standpoint to capture any oscillations that may occur in the flow. However, this method will be costly with respect to computation time and is not guaranteed to yield a correct solution. In any case, the 60 foot box cut scenario deserves further study before results can be utilized as a reliable design tool.

Modeling Scrubbers using Fluent

In this section, a cylindrical scrubber was inserted into the 30 foot box cut geometry to represent experiments performed by Wala and Jacob. Results for these studies are presented in the annual report submitted by Dr. Wala to NIOSH in 2003. In these studies, the scrubber mass flow ratio is normalized by the mass flow at the inlet, or behind the curtain. Thus, the results presented in figures 17 through 21 illustrate predicted flow fields at scrubber mass flow ratios of 0.2, 0.3, 0.4, 0.7 and 1.0, respectively. The boundary condition for the scrubber is set as a constant velocity outlet which is released outside the original geometry. This boundary condition is set by the apparatus available to Wala for PIV experimentations. The grid density was based on the coarse grids simulated in the previous section. It should be noted that a grid-independent solution has not been found for these results due to time constraints.

In comparing the results shown in this report with the PIV results presented by Wala, one will notice a discrepancy. Wala's experiments show the location of the separation point to be more sensitive to smaller values of the scrubber mass flow ratio. However, once the scrubber mass flow ratio reaches a level near 1.0 the separation is removed and the flow carries to the cutting face. Since most scrubbers in actual mining applications are required to have a mass flow ratio greater than or equivalent to 1.0, one could argue that Fluent's predictions are accurate within the range of applicable problems. However, users of Fluent as a design tool should make note of the limitations that are found in this study when applying Fluent to scenarios beyond or on the borders of this range. A potential scenario that should be avoided is an attempt to reduce the requirement for the scrubber mass flow rate for the purpose of using smaller, less expensive blowers.

Modeling a Continuous Miner with On-board Scrubbers using Fluent

Once CFD is validated for benchmarked applications, the strength of CFD can be fully utilized. Prior to this section, the geometries of the models presented in this report can be regarded as "simple". Thus, experimentation seems to be a more effective and productive means of study. However, these simplified geometries are used as benchmarks to validate the CFD codes for use in more realistic applications. Because CFD does not require a model shop, geometries are no longer time consuming to build, relative to the time it takes to generate a precise scale model of intricate detail. Geometries can be imported directly from 3-D solid modeling software or manually generated in Gambit, Fluent's grid generation package. Also, the CFD user has access to many more boundary conditions than the experimentalist at a fraction of the cost. For example, study the flow over a continuous miner with scrubbers on-board is a much easier and less expensive task for a CFD user than for an experimentalist. The experimentalist would be forced to make a decision between a full-scale model and a scaled model. To put an actual continuous miner in a full scale mine and set up the measuring devices would be expensive and time consuming. Building a scaled miner and mine using a rapid prototyping technique and setting up the measurement apparatus would also be somewhat less expensive but still time consuming. However, dumping a 3-D rendering of the miner into a virtual mine, generating a grid and running the simulation with the appropriate boundary conditions would take an experienced CFD user a matter of weeks and cost of only the software and hardware. Furthermore, once the software and hardware are paid for, they can be re-used for other models. The power of CFD now becomes apparent, but more work must be done to ensure the quality of the solutions it generates.

The results in this section provide a look ahead to see some of the possibilities that CFD has to offer. In these simulations, a simplified virtual continuous miner was inserted into the mine for the 30 foot box cut scenario. Figures 22 and 23 show different views of the virtual geometry. The miner is equipped with a virtual scrubber which is incorporated into the geometry of the mine such that the scrubber's inlets are placed on each side of the miner and the exhaust is placed at its rear. Unlike the previous scrubber, this scrubber is modeled with the "fan" UDF (User Defined Function) available in Fluent. This method of modeling allows the user to put a pressure gradient condition on a plane within the scrubber's duct essentially modeling a blower mounted to the miner. The main difference between this method and the previously used method is that the scrubber's exhaust is released within the mine as opposed to outside. This better represents the scenario of a miner with on-board scrubber and would be very difficult for an experimentalist to implement into a scaled model due to flow restrictions on fans small enough to fit these models. One downside to using the "fan" UDF is that the input is a pressure gradient which cannot be directly related to a mass flow rate without first solving the flow field. However, within a matter of four simulations, a scrubber mass flow ratio, normalized by the inlet mass flow as before, of 0.95 is reached.

Figure 24 illustrates the resulting flow over the miner without the use of a scrubber. The effect of the scrubber can be seen by comparing figures 25 through 28 with figure 24. The corresponding scrubber mass flow ratios for figures 25, 26, 27 and 28 are 0.37, 0.67, 0.83 and 0.95, respectively.

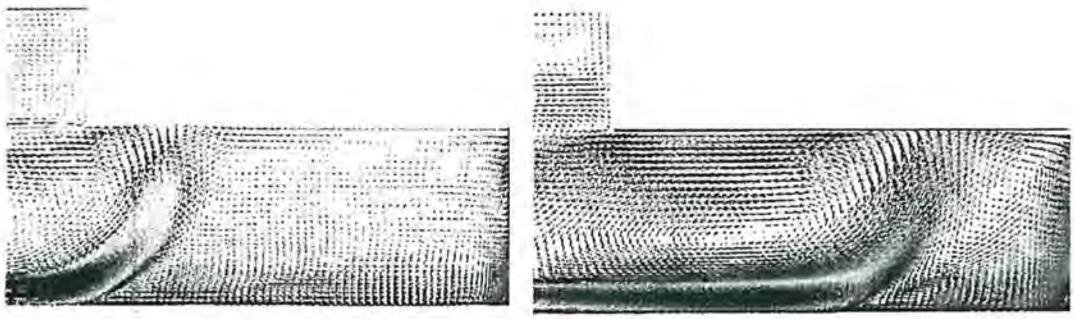

Figure 5: Velocity vectors for 30 foot box cut using Fluent (left) and CFX (right) with a coarse grid.

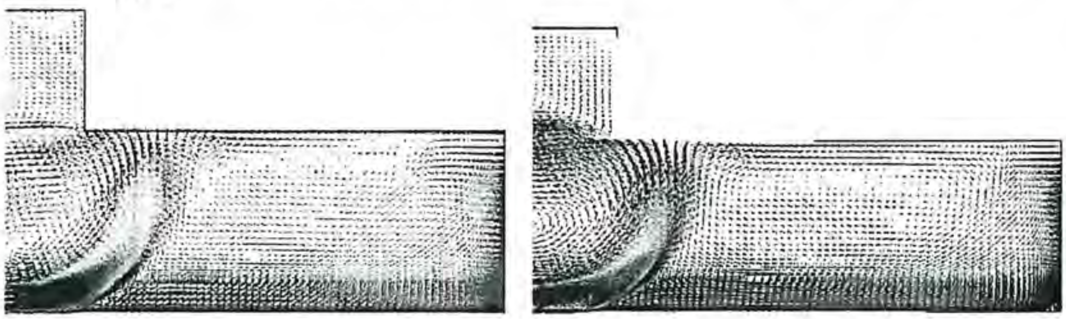

Figure 6: Velocity vectors for 30 foot box cut using Fluent (left) and CFX (right) with a moderate grid.

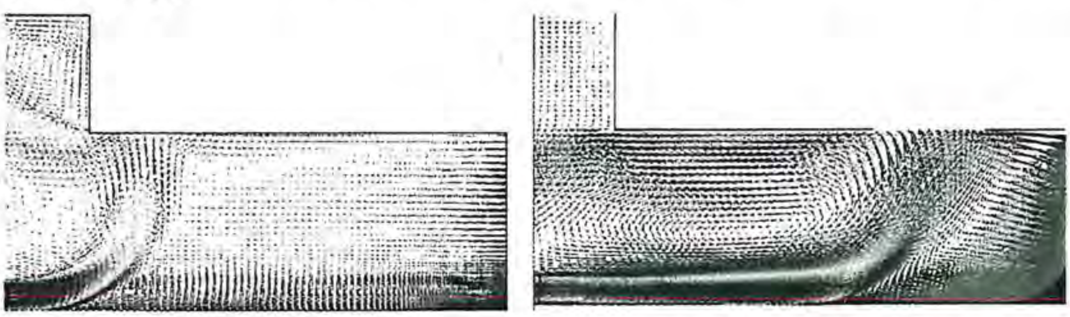

Figure 7: Velocity vectors for 30 foot box cut using Fluent (left) and CFX (right) with a fine grid.

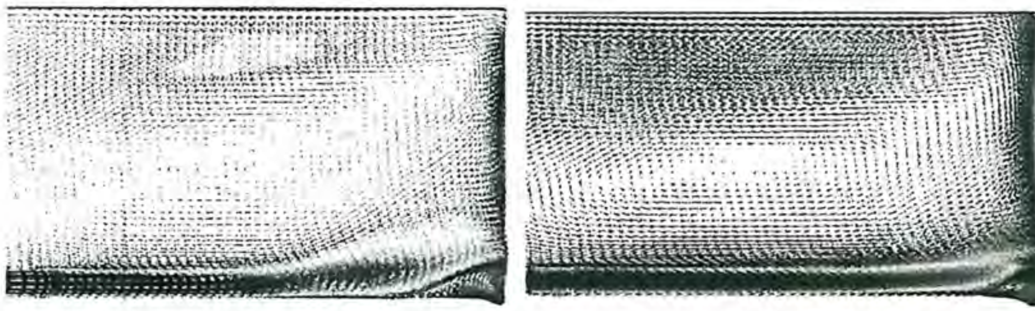

Figure 8: Velocity vectors for 30 foot slab cut using Fluent (left) and CFX (right) with a coarse grid.

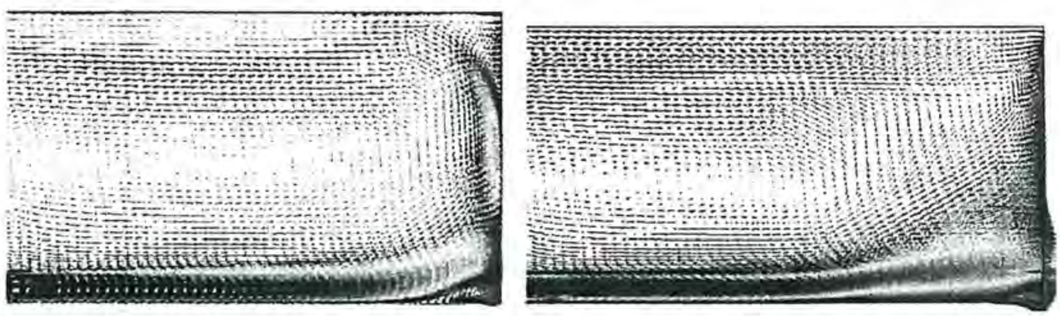

Figure 9: Velocity vectors for 30 foot slab cut using Fluent (left) and CFX (right) with a moderate grid.

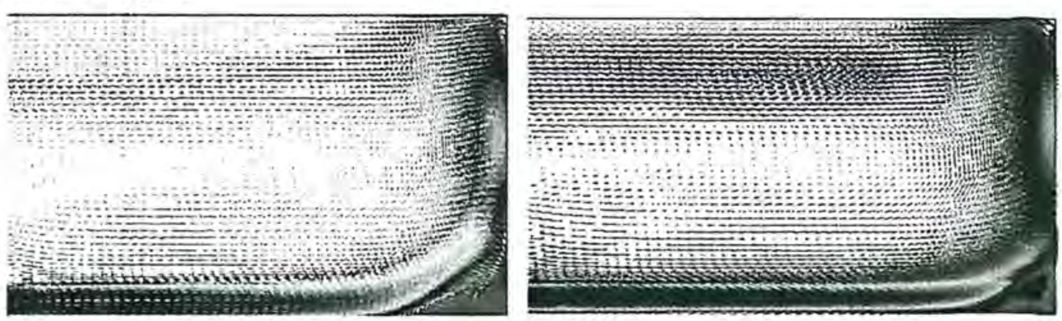

Figure 10: Velocity vectors for 30 foot slab cut using Fluent (left) and CFX (right) with a fine grid.

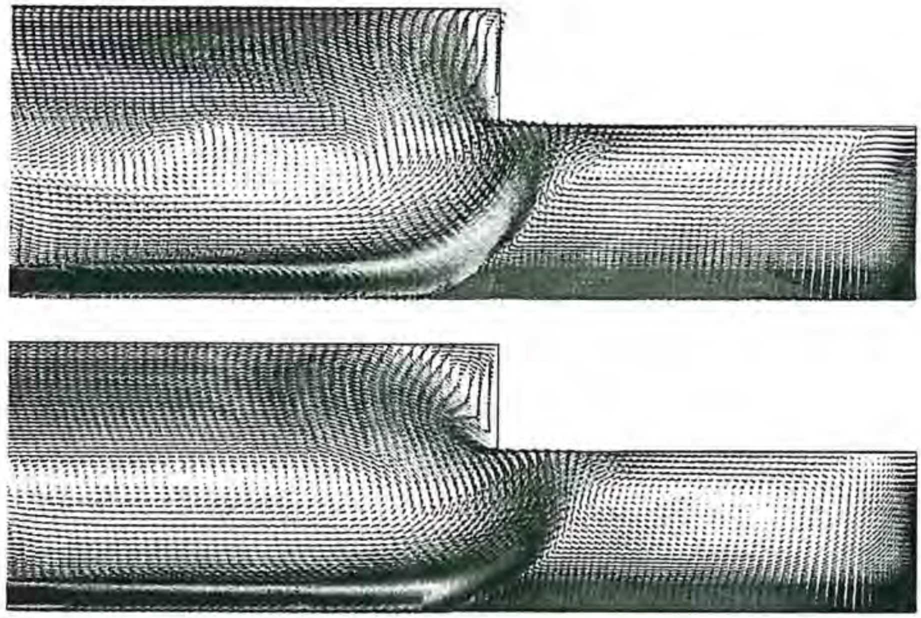

Figure 11: Velocity vectors for 60 foot box cut using Fluent (top) and CFX (bottom) with a coarse grid.

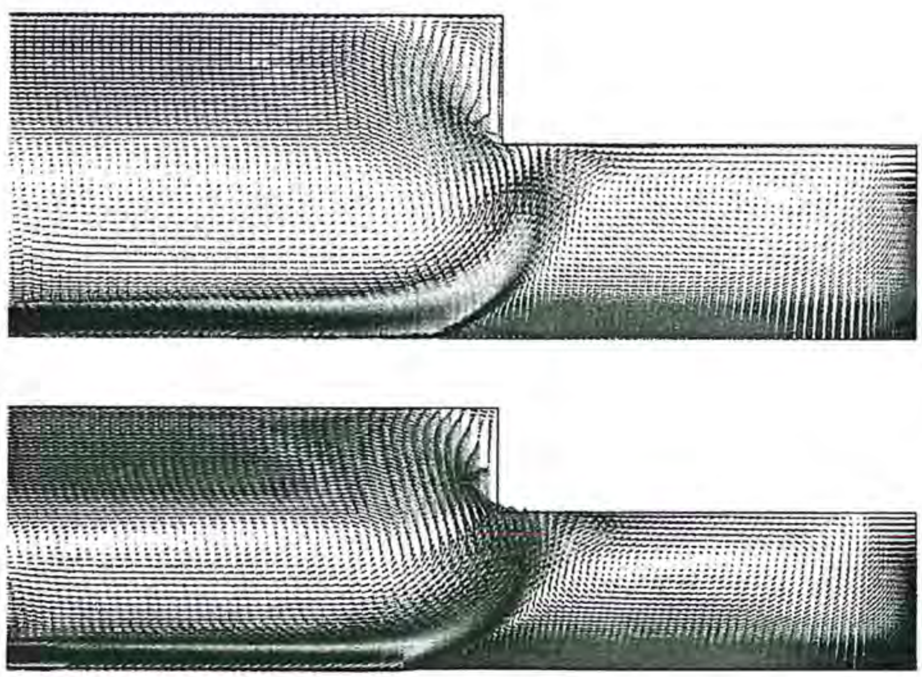

Figure 12: Velocity vectors for 60 foot box cut using Fluent (top) and CFX (bottom) with a moderate grid.

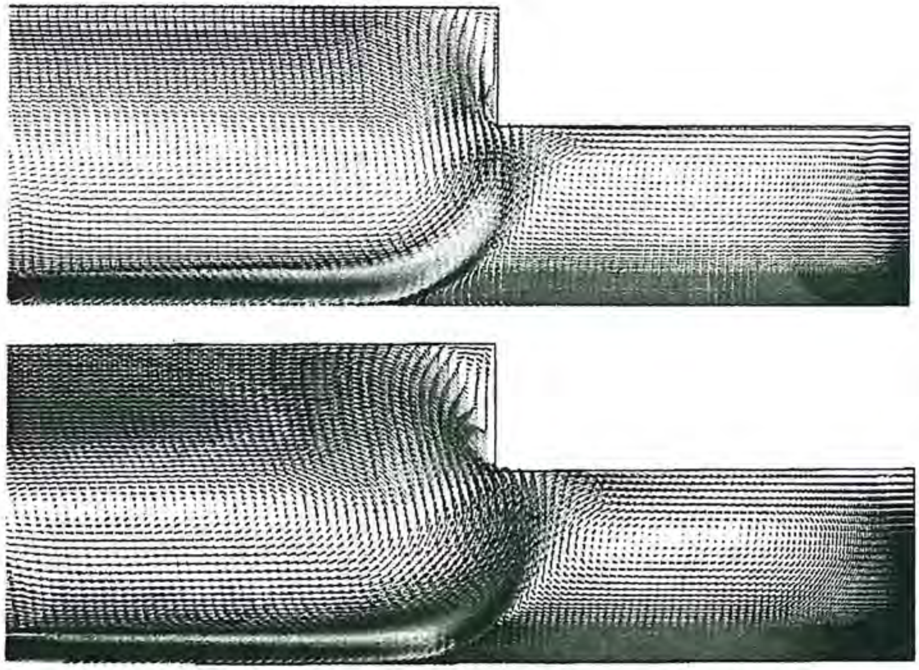

Figure 13: Velocity vectors for 60 foot box cut using Fluent (top) and CFX (bottom) with a fine grid.

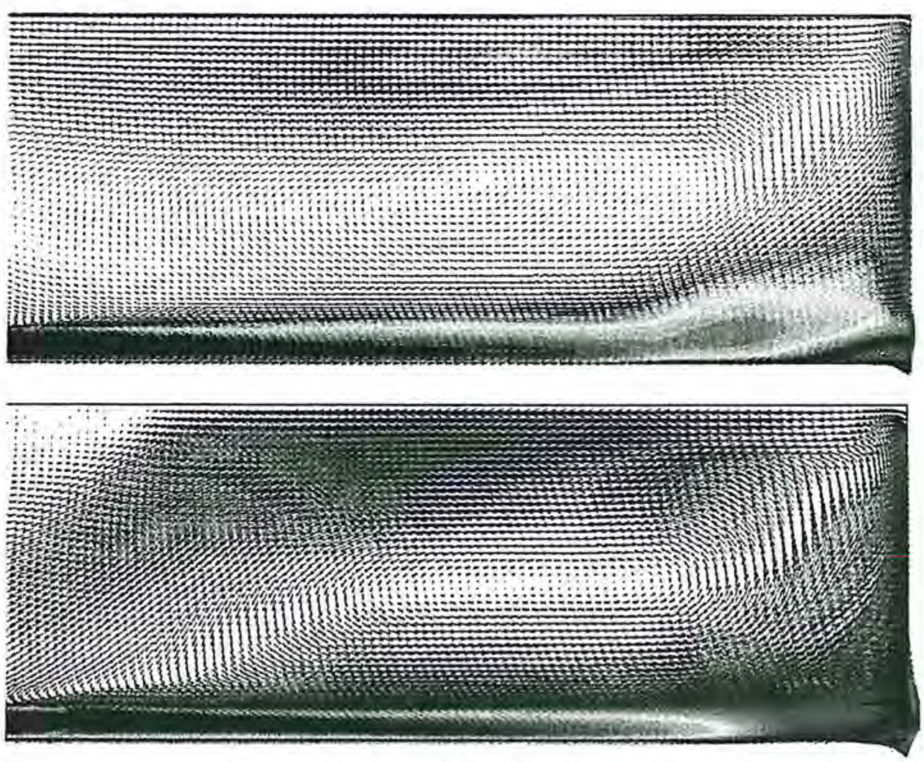

Figure 14: Velocity vectors for 60 foot slab cut using Fluent (top) and CFX (bottom) with a coarse grid.

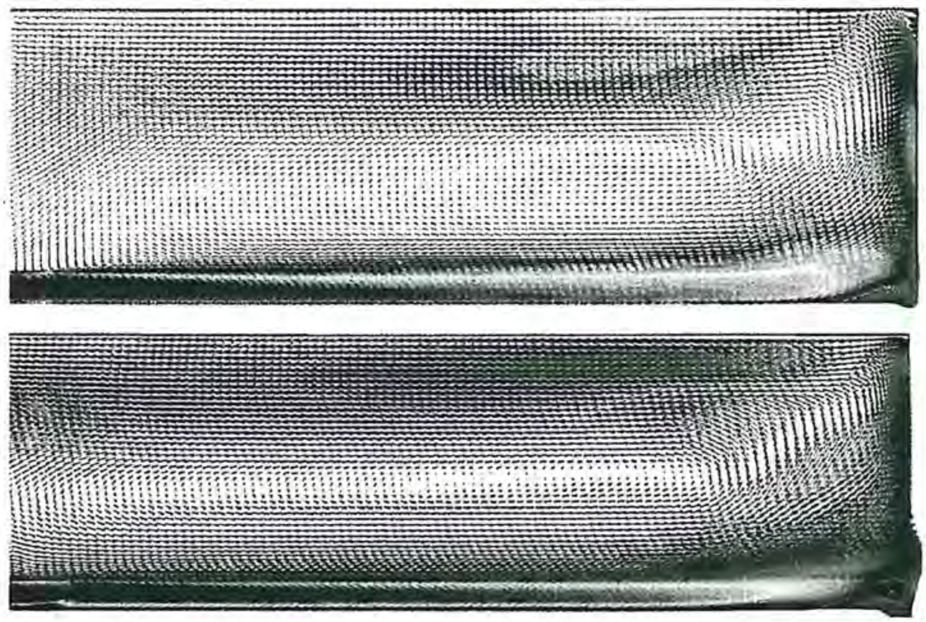

Figure 15: Velocity vectors for 60 foot slab cut using Fluent (top) and CFX (bottom) with a moderate grid.

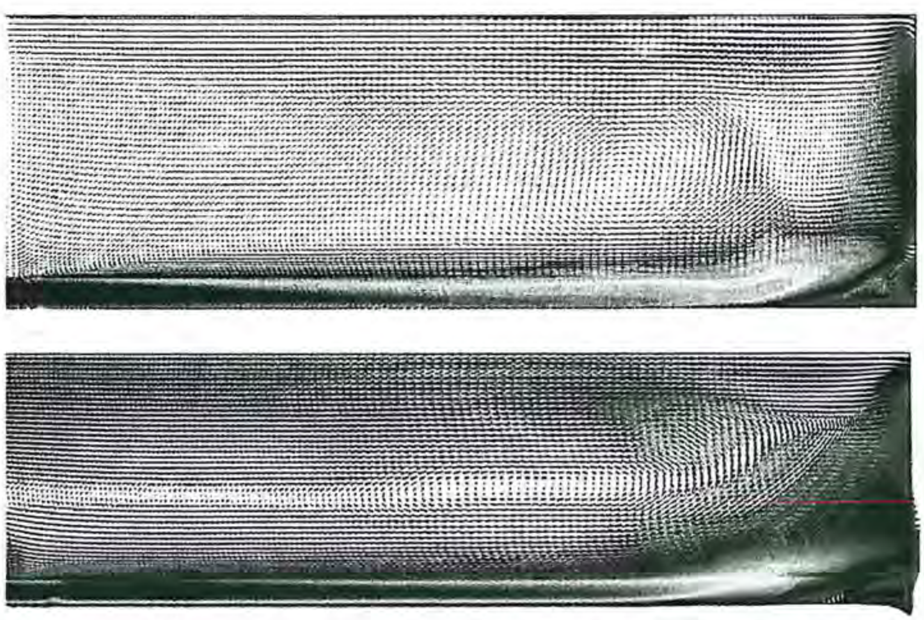

Figure 16: Velocity vectors for 60 foot slab cut using Fluent (top) and CFX (bottom) with a fine grid.

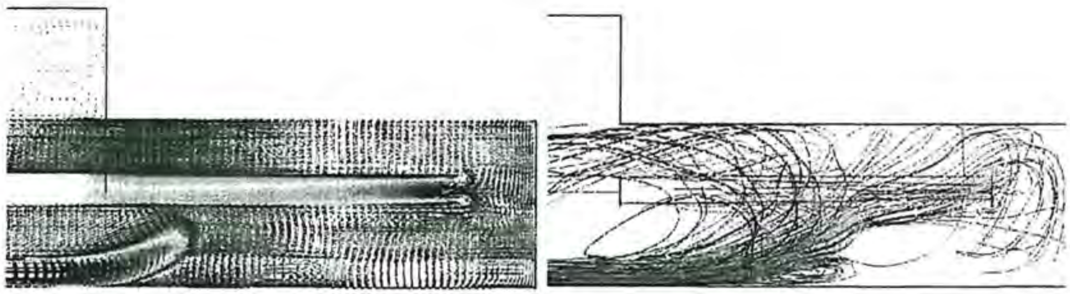

Figure 17: (Left) Velocity vectors in the Scrubber Plane and (right) path lines from the top view for the 30 foot box cut scenario with scrubber mass flow ratio of 20%.

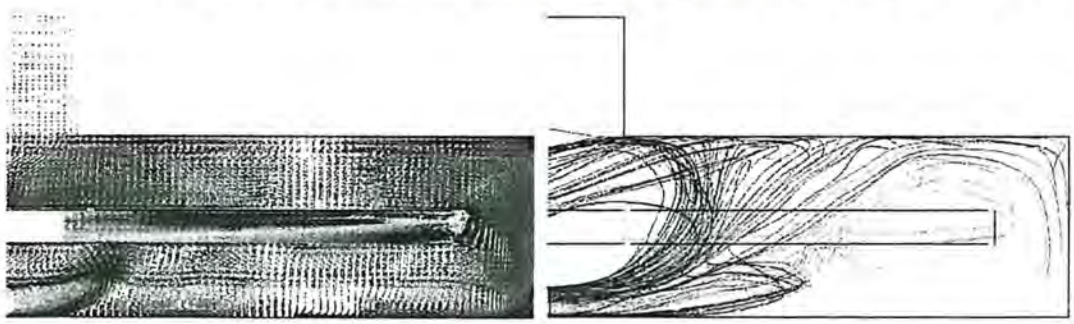

Figure 18: (Left) Velocity vectors in the Scrubber Plane and (right) path lines from the top view for the 30 foot box cut scenario with scrubber mass flow ratio of 30%.

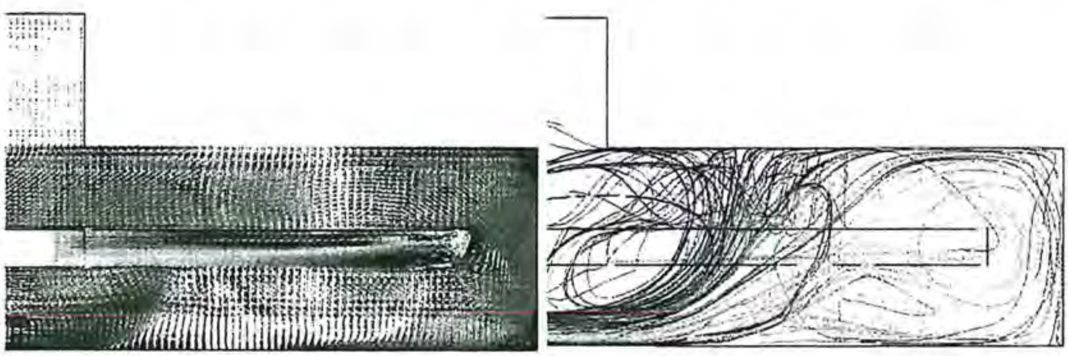

Figure 19: (Left) Velocity vectors in the Scrubber Plane and (right) path lines from the top view for the 30 foot box cut scenario with scrubber mass flow ratio of 40%.

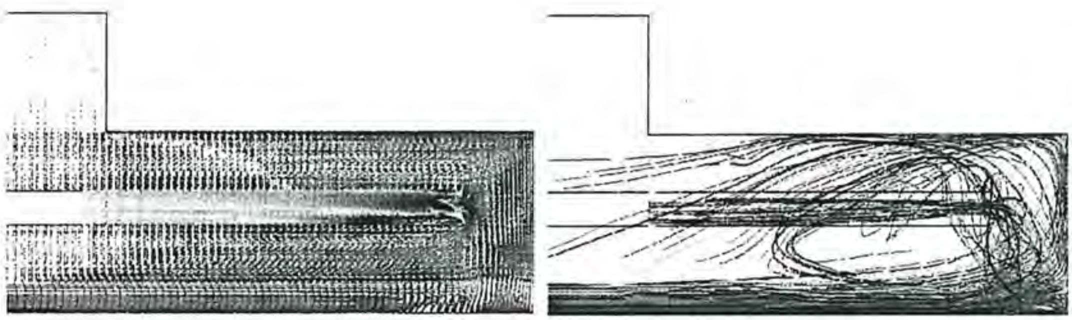

Figure 20: (Left) Velocity vectors in the Scrubber Plane and (right) path lines from the top view for the 30 foot box cut scenario with scrubber mass flow ratio of 70%.

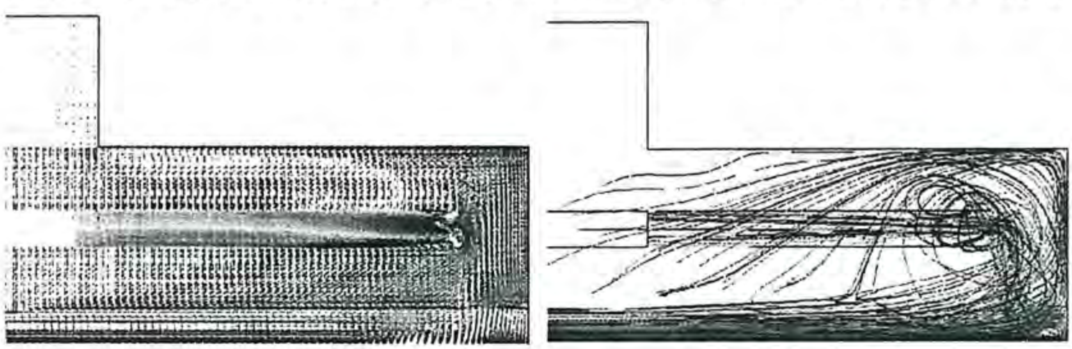

Figure 21: (Left) Velocity vectors in the Scrubber Plane and (right) path lines from the top view for the 30 foot box cut scenario with scrubber mass flow ratio of 100%.

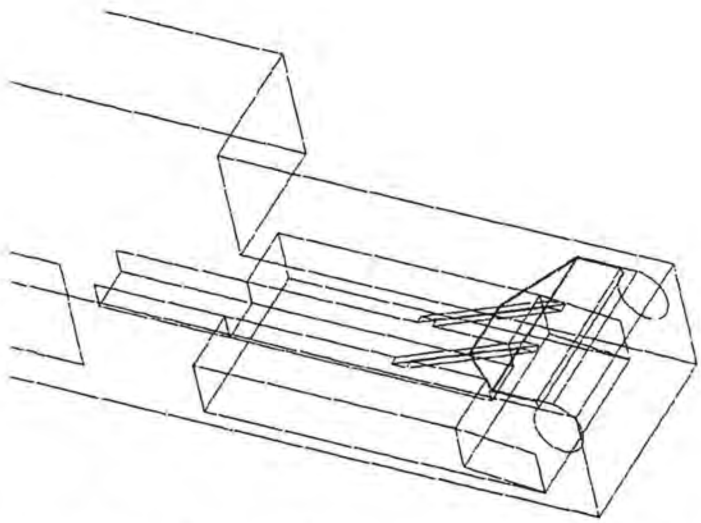

Figure 22: Isometric view of a simplified representation of a continuous miner inserted into the 30 foot box cut scenario.

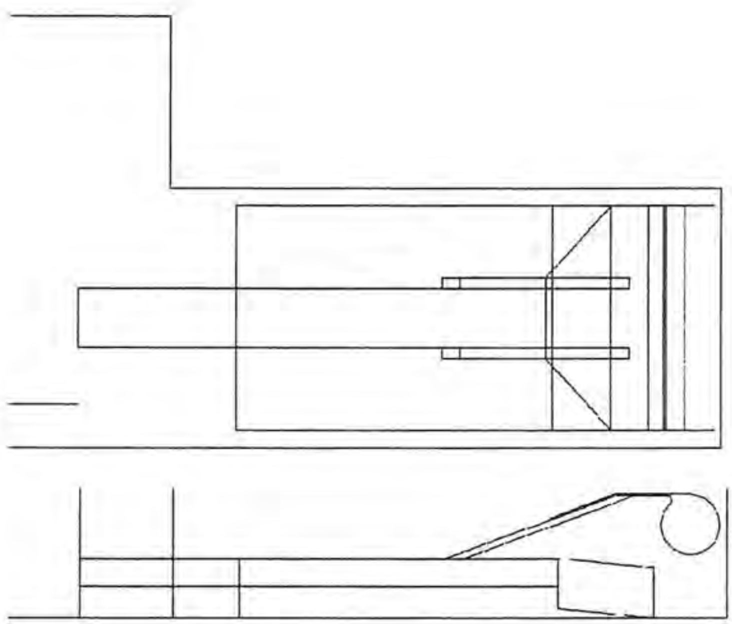

Figure 23: A top view (top) and a side view (bottom) of a simplified representation of a continuous miner inserted into the 30 foot box cut scenario.

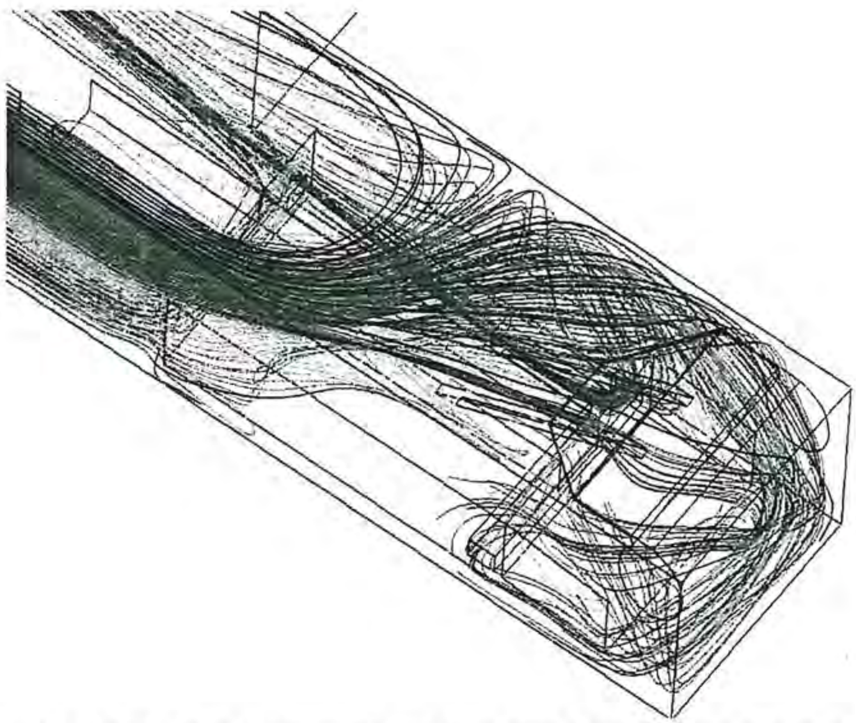

Figure 24: 3-D path lines illustrating the flow over a continuous miner in the 30 foot box cut scenario without a scrubber.

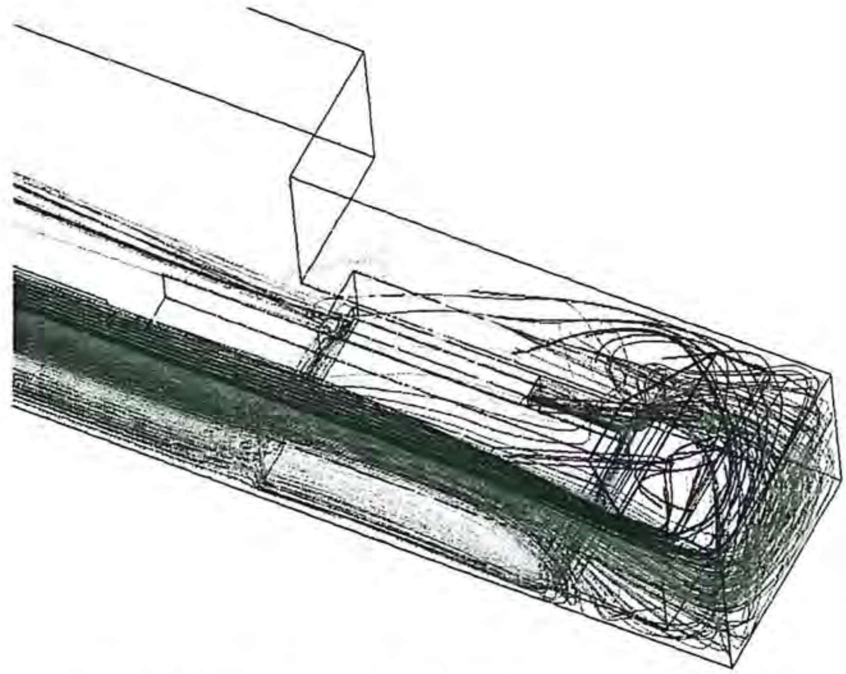

Figure 25: 3-D path lines illustrating the flow over a continuous miner in the 30 foot box cut scenario with a scrubber mass flow ratio of 0.37.

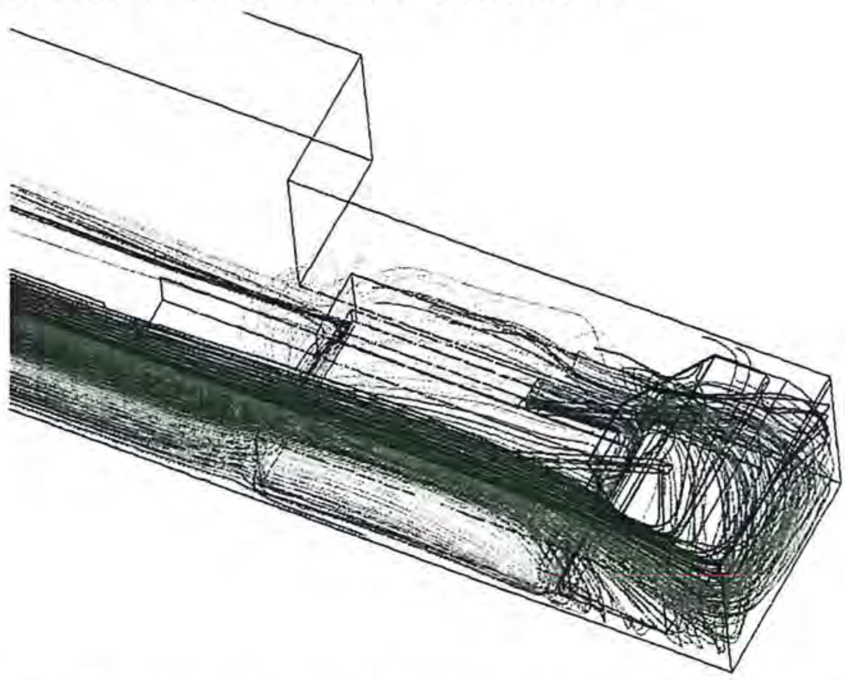

Figure 26: 3-D path lines illustrating the flow over a continuous miner in the 30 foot box cut scenario with a scrubber mass flow ratio of 0.67.

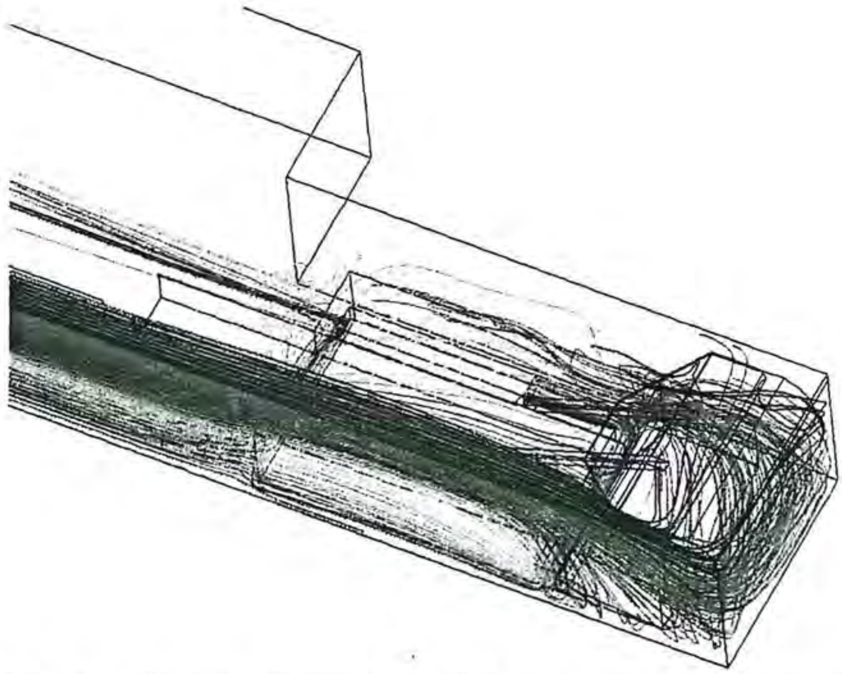

Figure 27: 3-D path lines illustrating the flow over a continuous miner in the 30 foot box cut scenario with a scrubber mass flow ratio of 0.83.

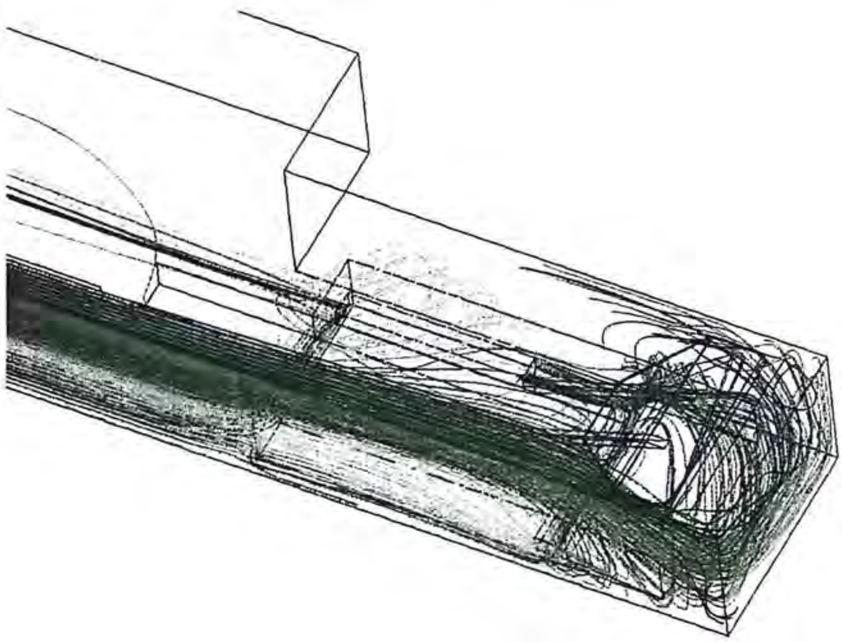

Figure 28: 3-D path lines illustrating the flow over a continuous miner in the 30 foot box cut scenario with a scrubber mass flow ratio of 0.95.